Electronic Supplementary Information

Chelation of Radium with Double-Armed Benzo-Rigidified Macrocycles for Radiopharmaceutical Purposes

Anastasia D. Zubenko,*[a] Anna V. Pashanova,[a] Lyubov S. Zamurueva,[b] Ekaterina V. Matazova,[b] Bayirta V. Egorova,[b] Ekaterina Y. Chernikova,[a] Valentina A. Karnoukhova,[a] Ivan V. Fedyanin,[a] Sofia P. Mosaleva, Yury V. Fedorov [a] and Olga A. Fedorova [a]

a. A. N. Nesmeyanov Institute of Organoelement Compounds of Russian Academy of Sciences, Vavilova St., 28, Moscow 119334, Russian Federation.

b. Lomonosov Moscow State University, Leninskie Gory, 1/3, Moscow 119991, Russian Federation.

* Email: zubenko@ineos.ac.ru

Content

1. Mass spectra of complexes

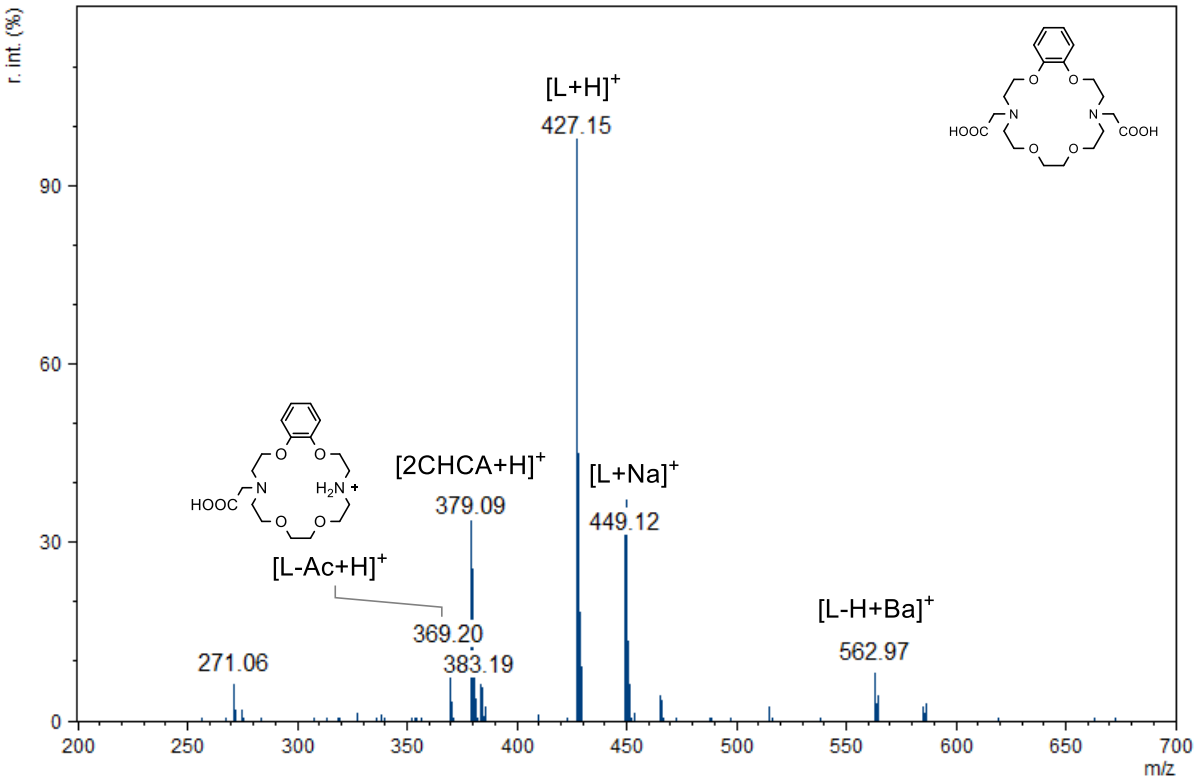

Figure S1. MALDI-TOF MS spectrum of BADA-18 in the presence of Ba^{2+} in H_2O using CHCA as a matrix.

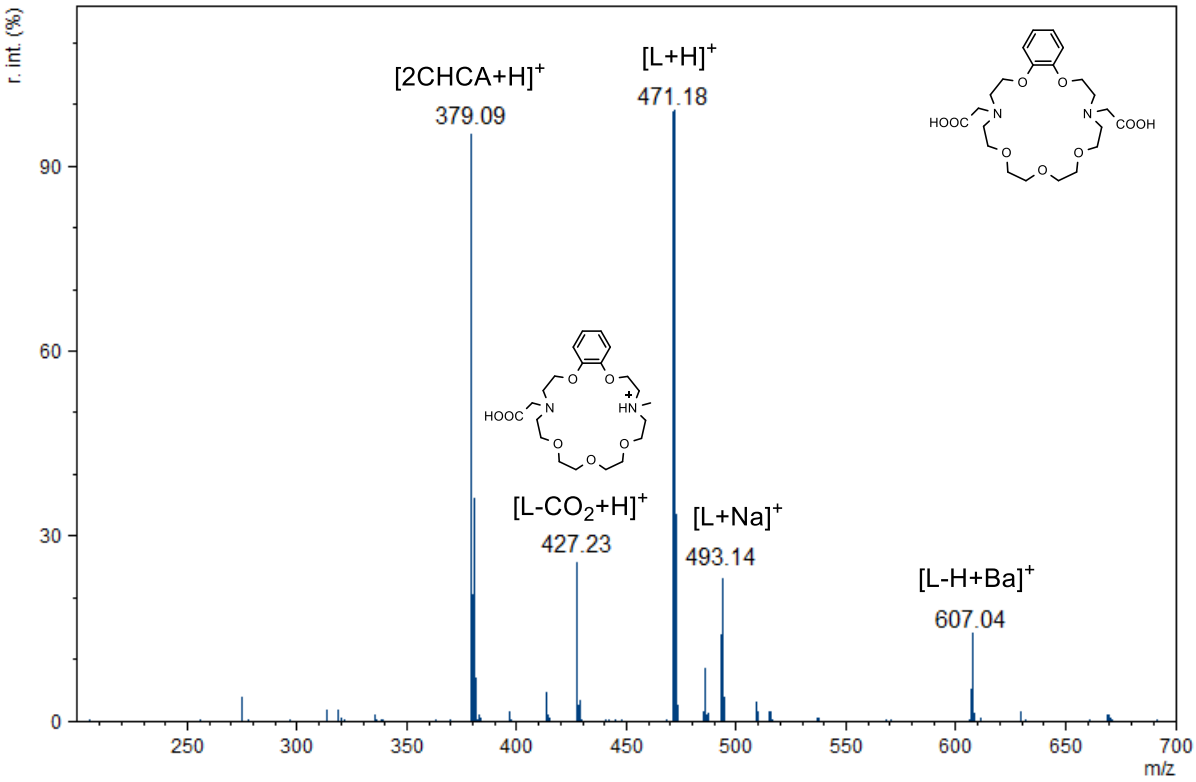

Figure S2. MALDI-TOF MS spectrum of BADA-21 in the presence of Ba^{2+} in H_2O using CHCA as a matrix.

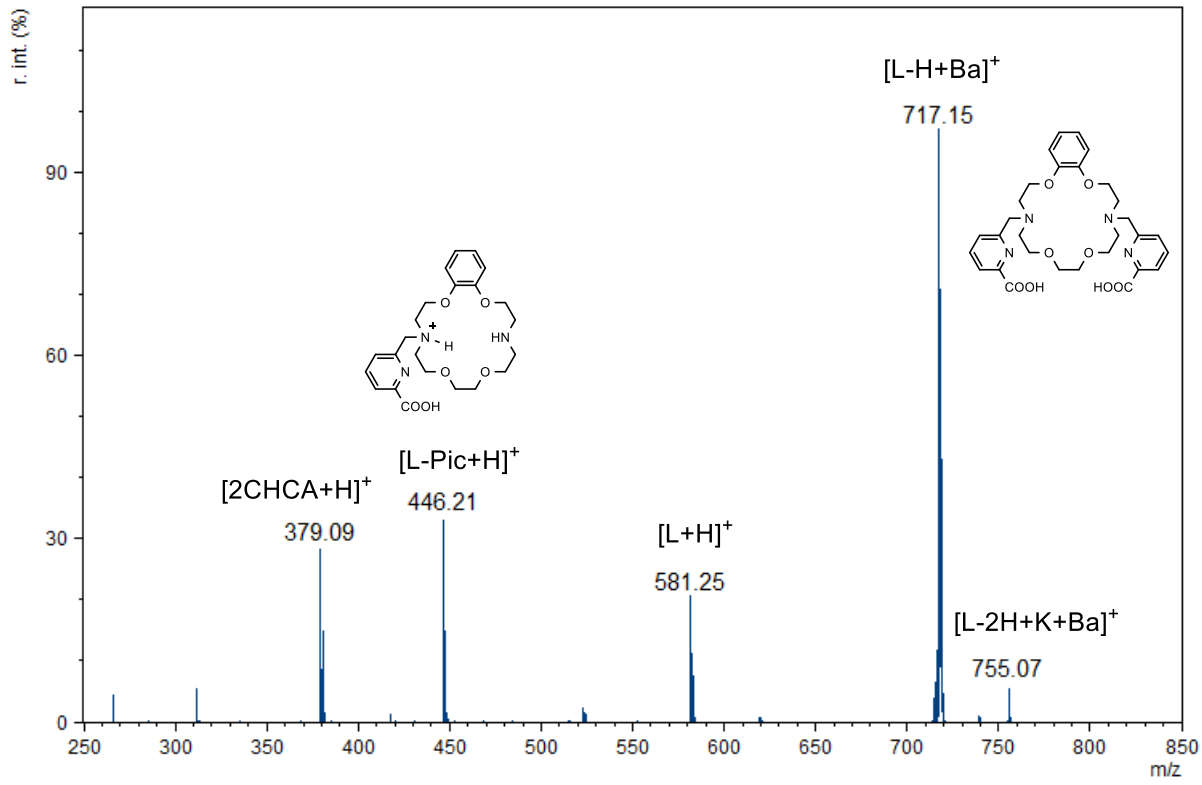

Figure S3. MALDI-TOF MS spectrum of BADPA-18 in the presence of Ba^{2+} in H_2O using CHCA as a matrix.

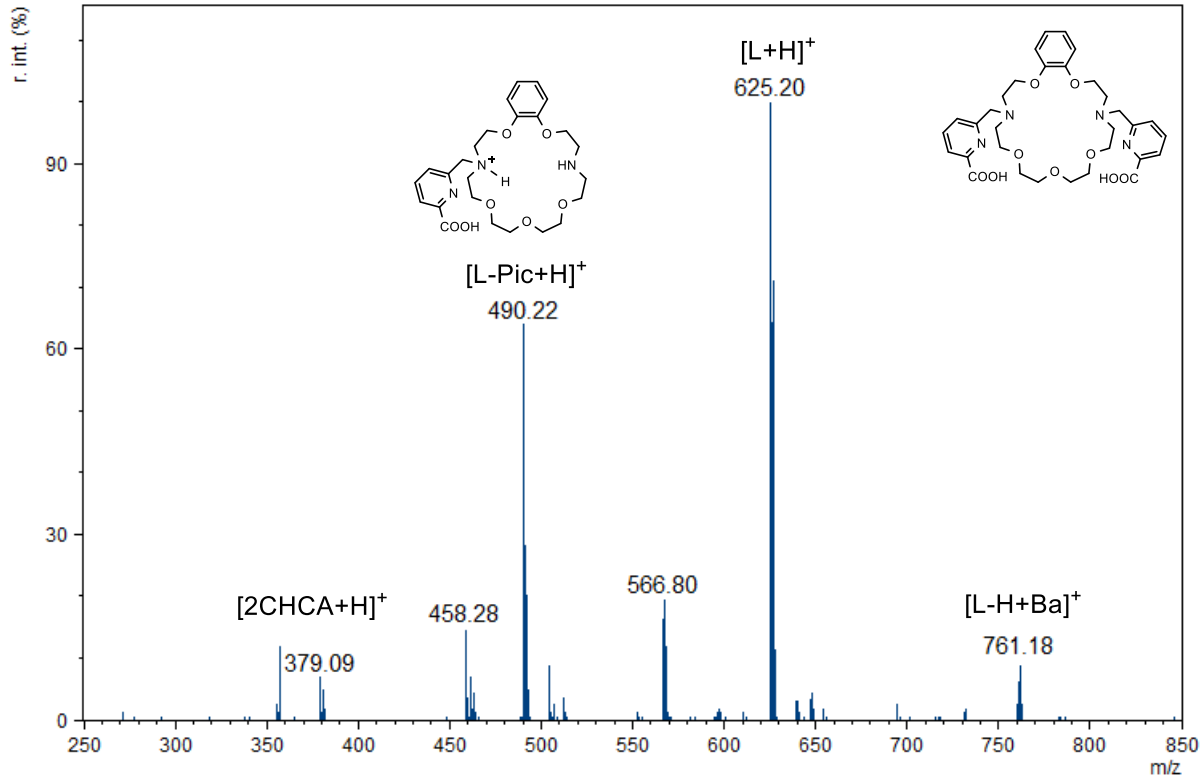

Figure S4. MALDI-TOF MS spectrum of BADPA-21 in the presence of Ba^{2+} in H_2O using CHCA as a matrix.

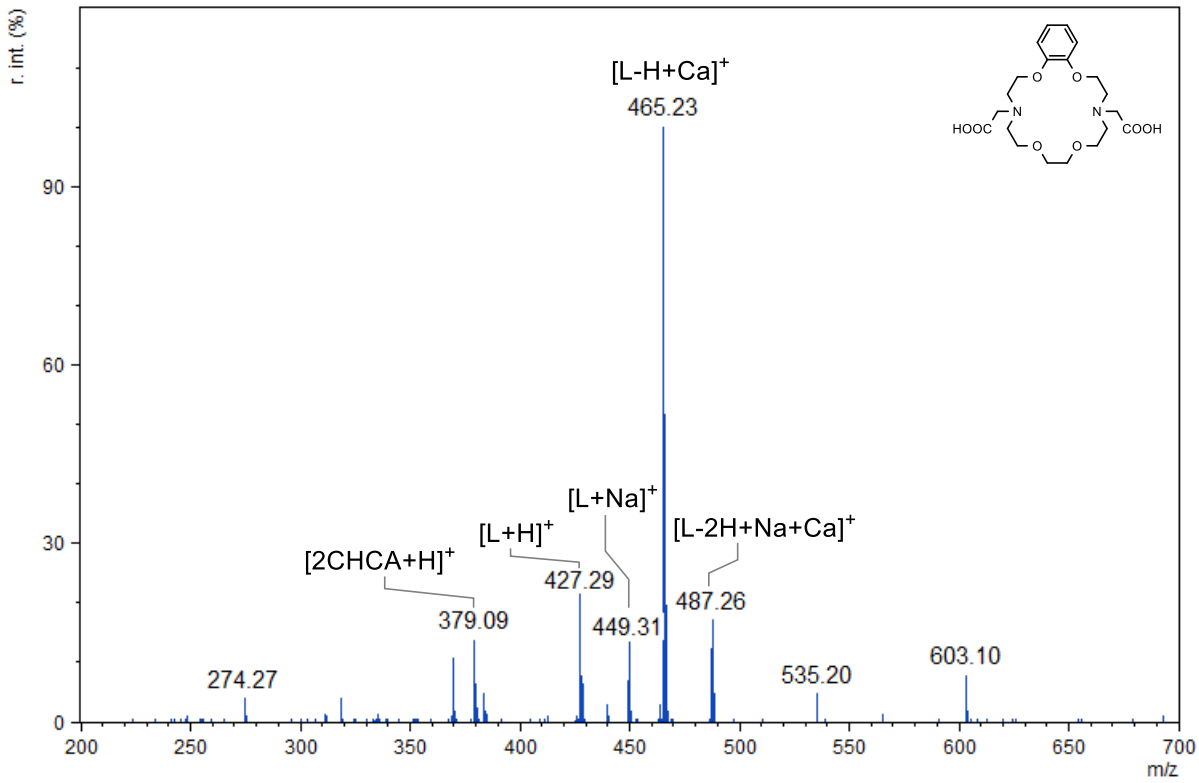

Figure S5. MALDI-TOF MS spectrum of BADA-18 in the presence of Ca^{2+} in H_2O using CHCA as a matrix.

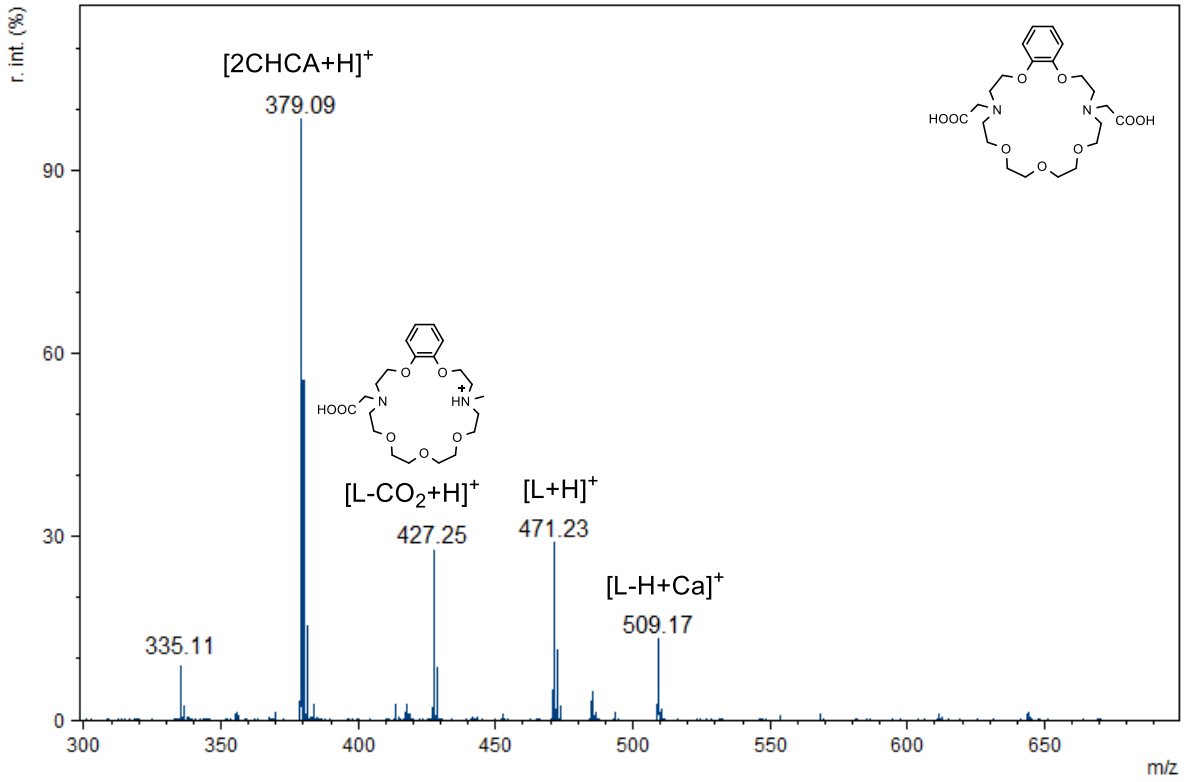

Figure S6. MALDI-TOF MS spectrum of BADA-21 in the presence of Ca^{2+} in H_2O using CHCA as a matrix.

2. Potentiometric titration

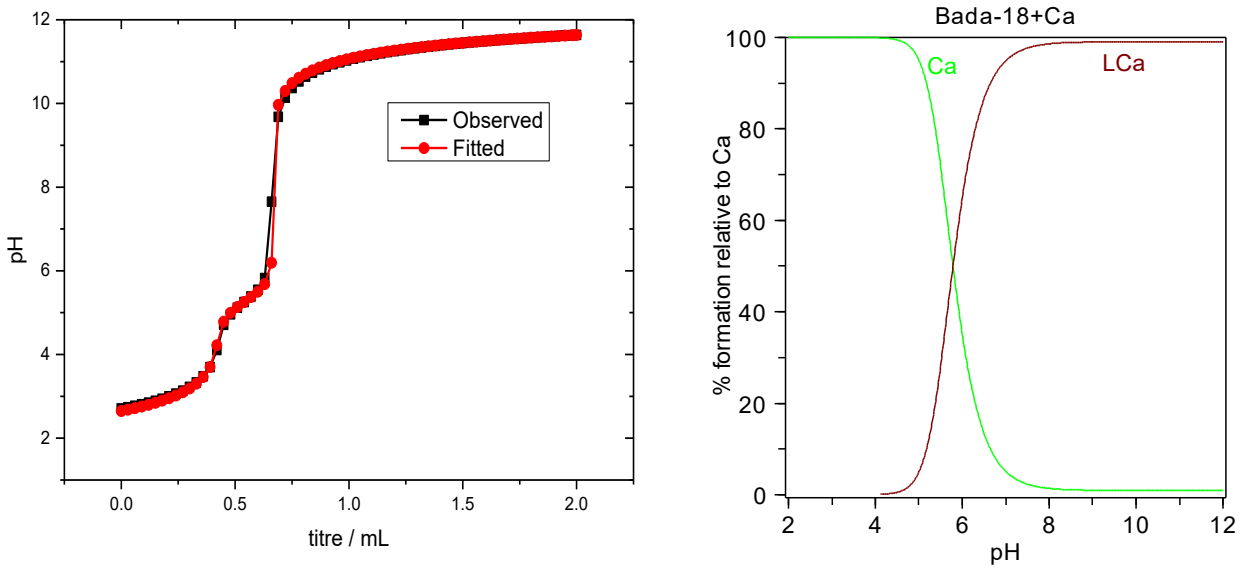

Figure S7. Potentiometric titration curves and species distribution diagram for the system Ca^{2+} (1 mM) and BADA-18 (1 mM) as a function of pH.

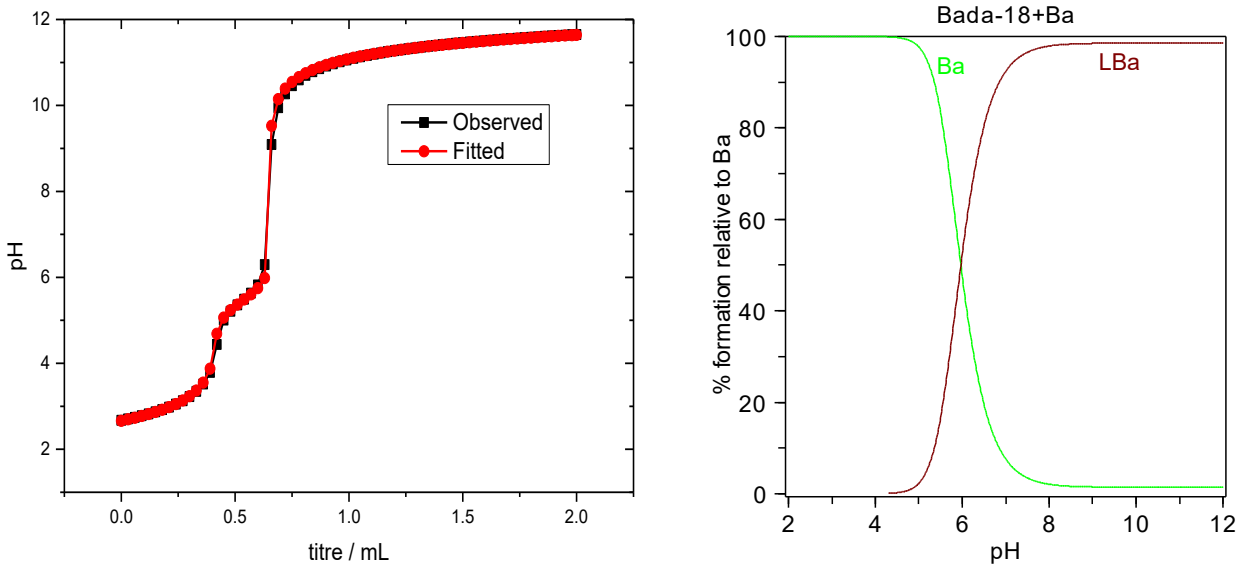

Figure S8. Potentiometric titration curves and species distribution diagram for the system Ba^{2+} (1 mM) and BADA-18 (1 mM) as a function of pH.

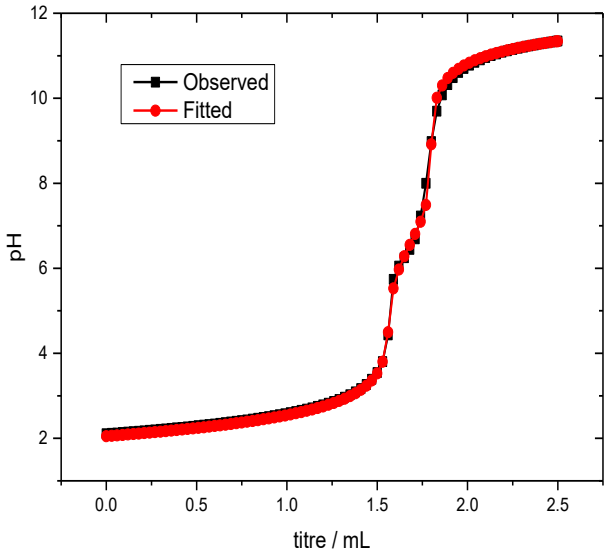

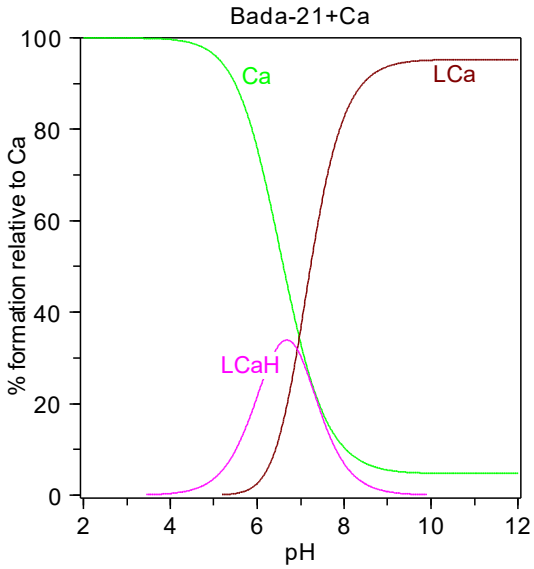

Figure S9. Potentiometric titration curves and species distribution diagram for the system Ca^{2+} (1 mM) and BADA-21 (1 mM) as a function of pH.

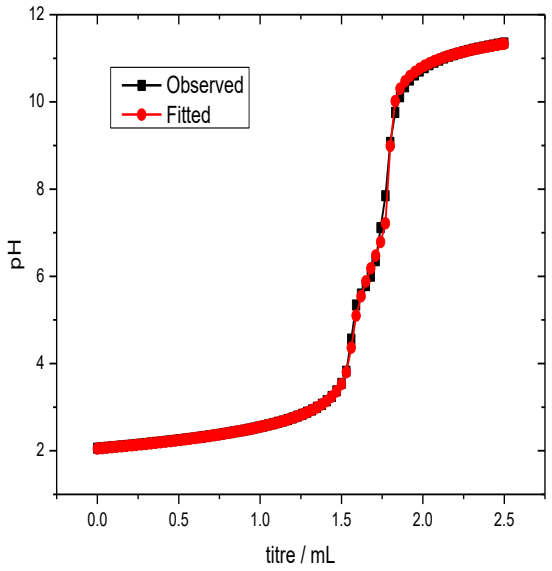

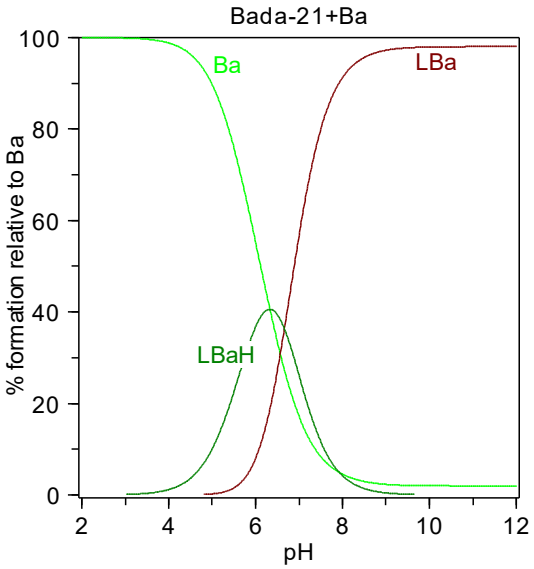

Figure S10. Potentiometric titration curves and species distribution diagram for the system Ba^{2+} (1 mM) and BADA-21 (1 mM) as a function of pH.

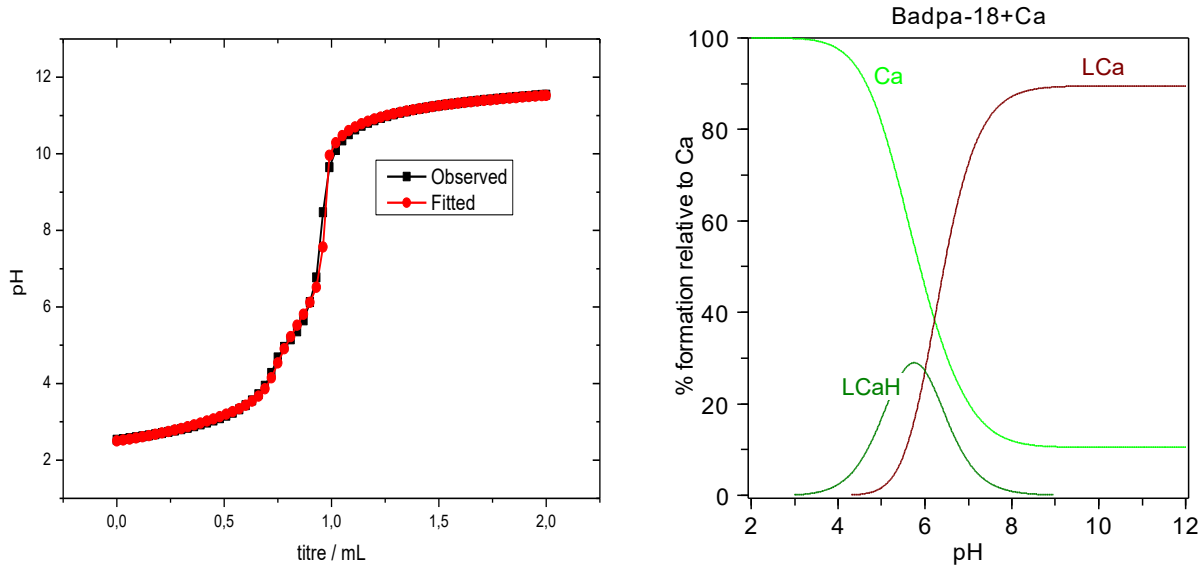

Figure S11. Potentiometric titration curves and species distribution diagram for the system Ca^{2+} (1 mM) and BADA-21 (1 mM) as a function of pH.

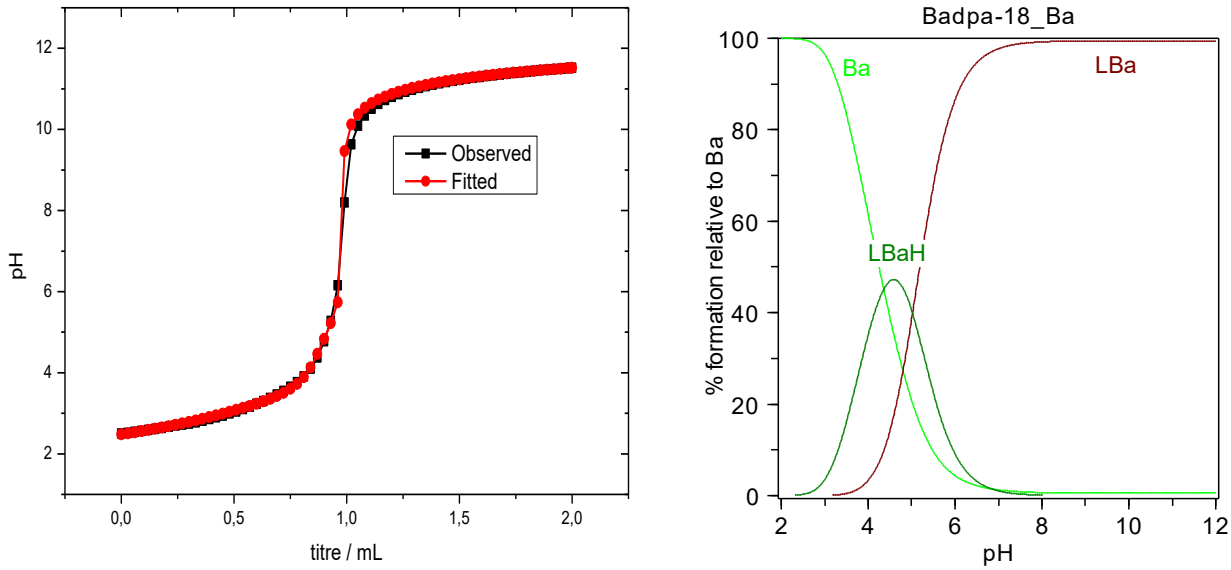

Figure S12. Potentiometric titration curves and species distribution diagram for the system Ba^{2+} (1 mM) and BADPA-18 (1 mM) as a function of pH.

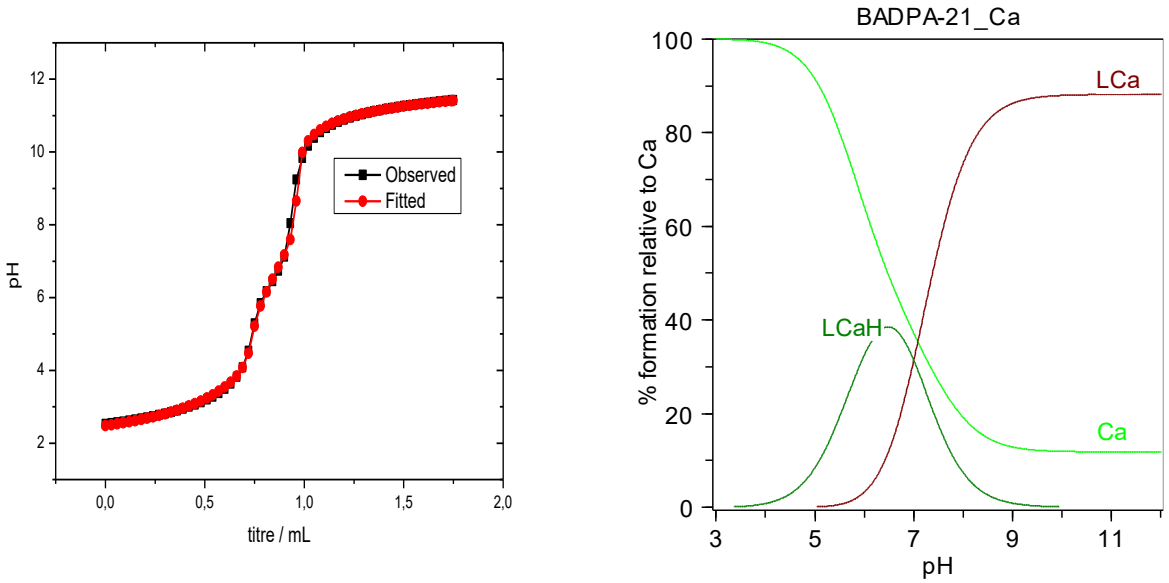

Figure S13. Potentiometric titration curves and species distribution diagram for the system Ca^{2+} (1 mM) and BADPA-21 (1 mM) as a function of pH.

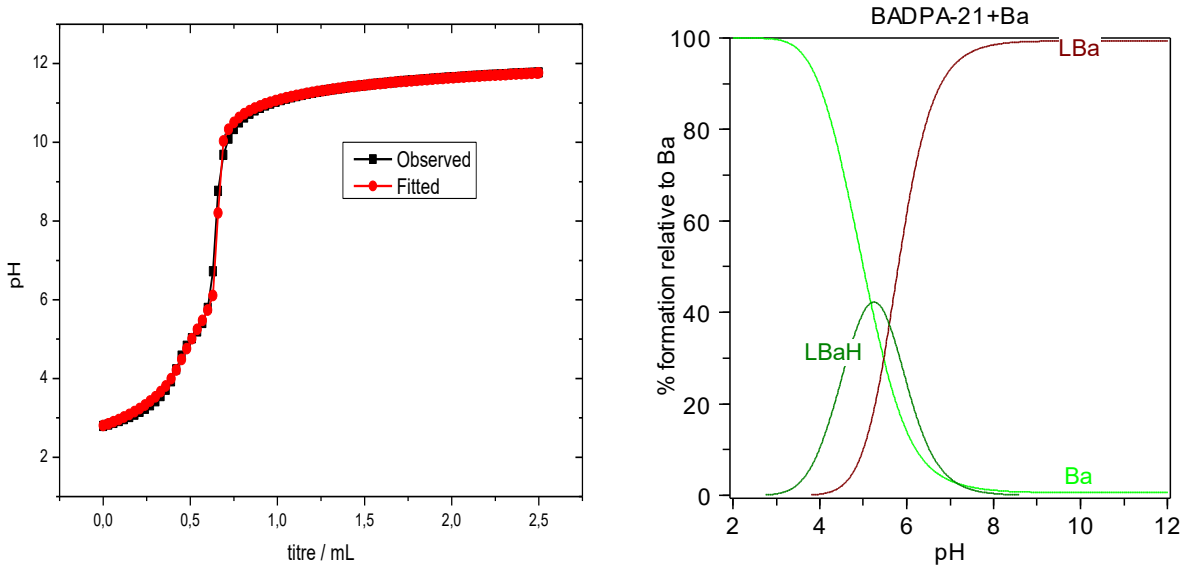

Figure S14. Potentiometric titration curves and species distribution diagram for the system Ba^{2+} (1 mM) and BADPA-21 (1 mM) as a function of pH.

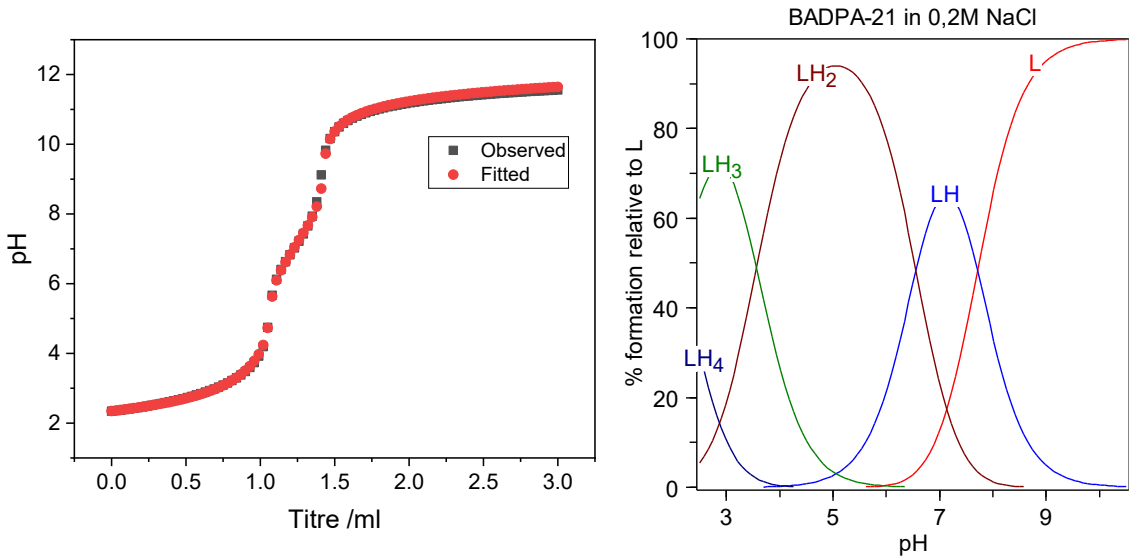

Figure S15. Potentiometric titration curves and species distribution diagram of BADPA-21 (1 mM) as a function of pH in 0.2 M NaCl.

Table S1. The protonation constants of BADPA-21 and macropa determined at 25 °C and I = 0.2 M NaCl.

	BADPA-21	Macropa [a]
LH	7.71(4)	7.94(2)
LH_2	6.57(4)	6.78(2)
LH_3	3.57(5)	3.29(4)
LH_4	2.17(5)	2.59(5)

[a] – Data from *Chem. Commun.*, 2022, 58, 9938–9941.

3. Cation exchange method

DATA treatment

The distribution coefficient D for sorption of resin can be expressed as:

$D = \frac{\sum[M]_{sorb}}{\sum[M]_{aq}}$ (1)

where M corresponds to Ra^{2+}.

For Ra^{2+} in the aqueous phase, the material balance equation is written as follows:

$[M]_{aq} = [M^{2+}] + [M(OH)^{1+}] + [ML]$ (2)

where L is BADPA-21 or macropa. The hydrolysis constant of Ra^{2+} is expressed as:

$K_{M(OH)} = \frac{[M(OH)]}{[M^{2+}][OH]}$ (3)

$[M]_{aq} = [M^{2+}]\left(1 + K_{M(OH)}[OH]\right) + [ML_n]$ (4)

Stability constants are defined as:

$\beta^{app} = \frac{[ML]}{[M^{2+}][L]^n}$ (5)

Hence, for (4):

$[M]_{aq} = [M^{2+}]\left(1 + K_{M(OH)}[OH]\right) + [M^{2+}]\beta^{app}[L]^n$ (6)

And finally:

$D = \frac{[\mathrm{M}]_{sorb}}{[M^{2+}]\left(1+K_{M(OH)}[OH]\right)+[M^{2+}]\beta^{app}[L]^n}$ (7)

The total concentration of ligand *c*(L) is expressed as:

$\mathrm{c}(L) = [L](1 + \sum_{m=1}^{4} K_{LH_m}[H]^m + \beta^{app}[M^{2+}])$ (8)

Taking into account the excess of the ligand compared to Ra^{2+}, we obtain:

$\frac{D_0}{D} = 1 + \frac{\beta_{app}(c(L))^n}{\left(1+K_{M(OH)}[OH]\right)\left(1+\sum_{m=1}^{4} K_{LH_m}[H]^m\right)}$ (9)

From the tangent of the slope of the (D_0/D – 1) dependence from c(L) the conditional stability constant can be obtained. Plotting in logarithmic coordinates $\lg\left(\frac{D_0}{D} - 1\right) = f\{lg(c(L))\}$ allow us to determine the stoichiometry of the complex by the tangent of the slope of the straight line, equal to *n*.

In current work we define conditional ("apparent") stability constants as:

$\beta^{app} = \beta_{101} + \beta_{111} \times [H^+]$ (10)

Where β_{101} corresponds to the stability constant of [RaL] form and β_{111} – to [RaHL].

Table S2. The L:M stoichiometry provided by the slope of the linear regression analysis of log (D_0/D-1) as a function of log *c*(L) for complexes with macropa and BADPA-21.

	pH	*c*(L), M	L:M ratio
macropa	5.9	$(1.78\text{-}17.8)\cdot10^{-6}$	1.09 ± 0.05
BADPA-21	6.5	$(4.44\text{-}35.6)\cdot10^{-5}$	1.01 ± 0.03
	7.0	$(5.33\text{-}26.7)\cdot10^{-5}$	0.95 ± 0.03
	7.5	$(0.889\text{-}13.3)\cdot10^{-5}$	0.98 ± 0.04

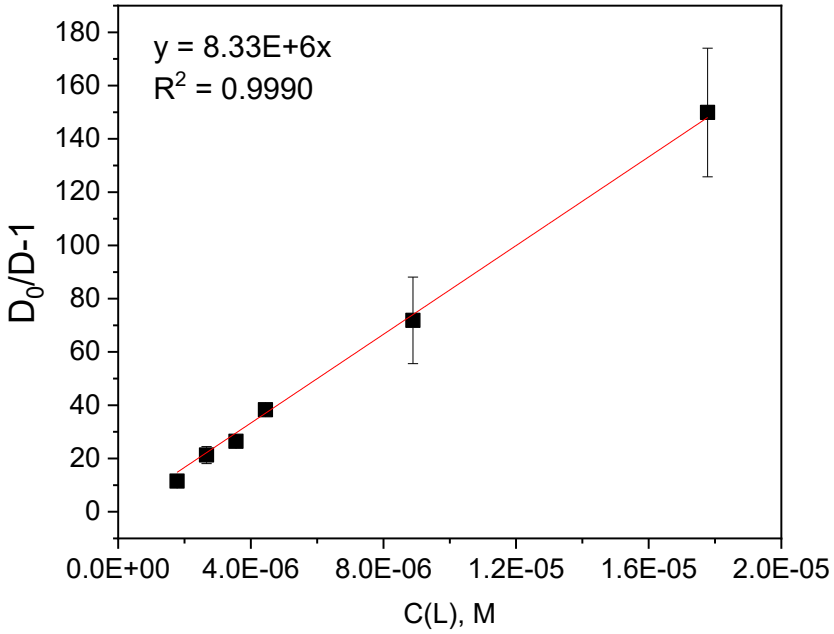

Figure S16. Determination of β_{app} for the Ra^{2+} complex with macropa from distribution data at pH 5.9. The value for log β_{app} provided by the slope of the linear fit is 9.9(1). The data represents the average of at least three replicates. Error bars are shown when the uncertainty is larger than the symbol in the plot.

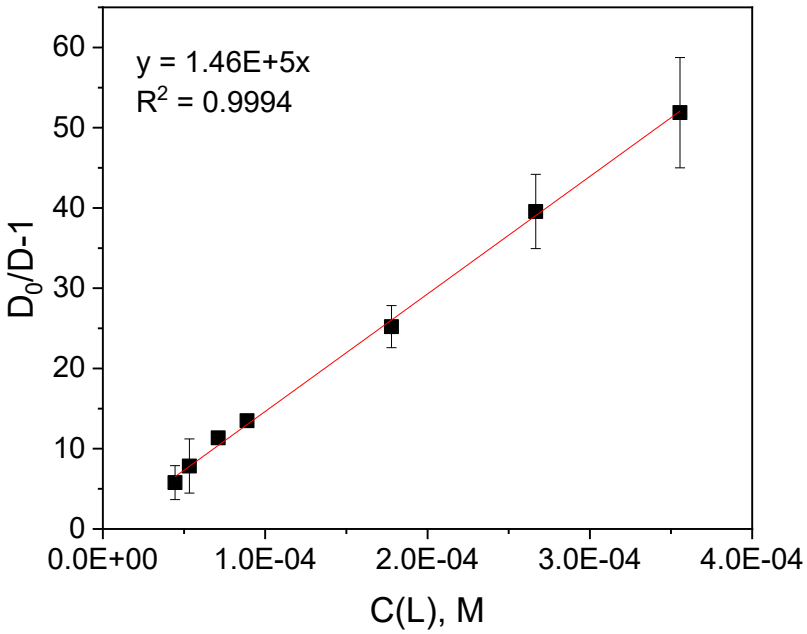

Figure S17. Determination of β_{app} for the Ra^{2+} complex with BADPA-21 from distribution data at pH 6.5. The value for log β_{app} provided by the slope of the linear fit is 6.72(8). The data represents the average of at least three replicates. Error bars are shown when the uncertainty is larger than the symbol in the plot.

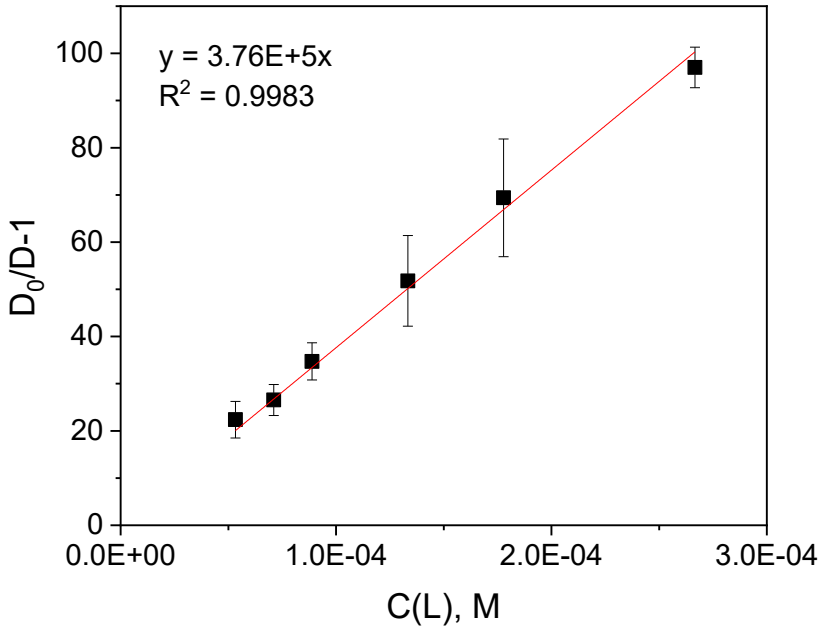

Figure S18. Determination of β_{app} for the Ra^{2+} complex with BADPA-21 from distribution data at pH 7.0. The value for log β_{app} provided by the slope of the linear fit is 6.5(1). The data represents the average of at least three replicates.

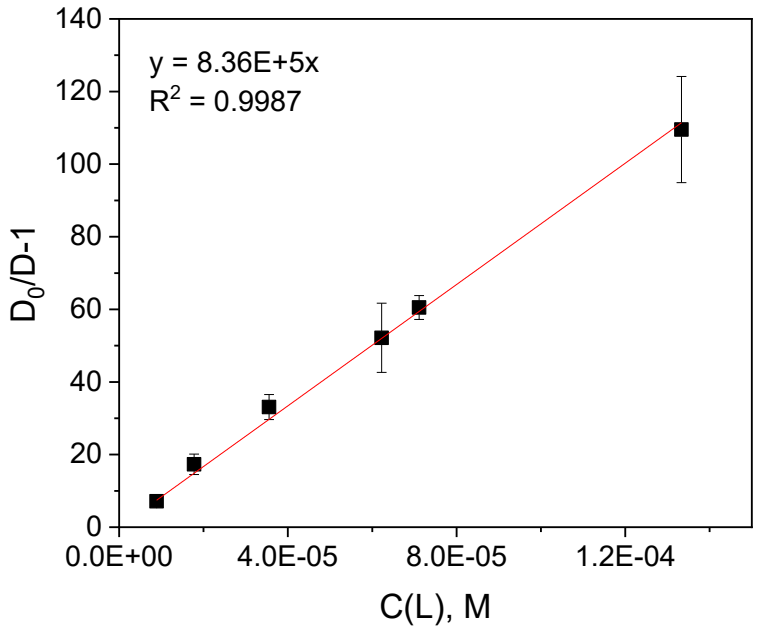

Figure S19. Determination of β_{app} for the Ra^{2+} complex with BADPA-21 from distribution data at pH 7.5. The value for log β_{app} provided by the slope of the linear fit is 6.4(1). The data represents the average of at least three replicates. Error bars are shown when the uncertainty is larger than the symbol in the plot.

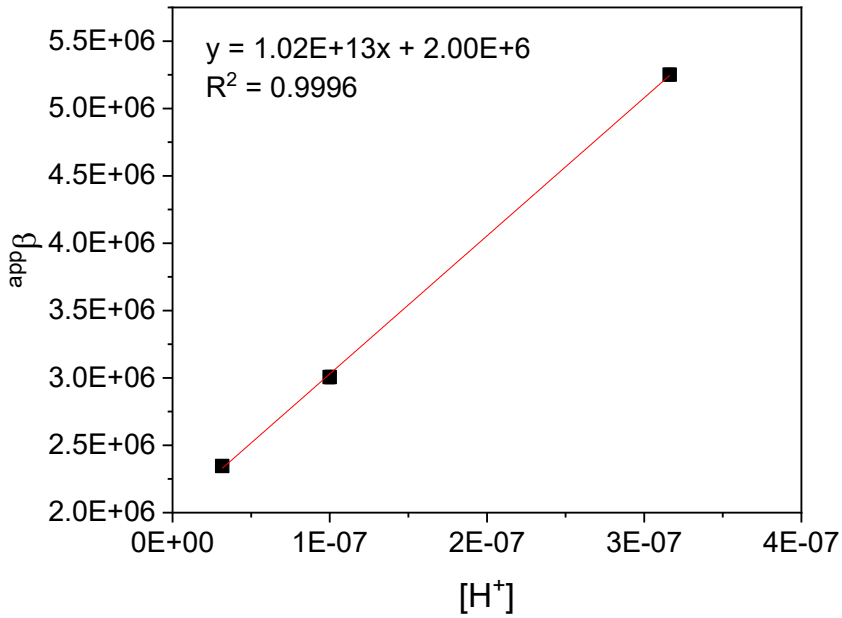

Figure S20. β_{app} dependence on [H^+]. Error bars are shown when the uncertainty is larger than the symbol in the plot.

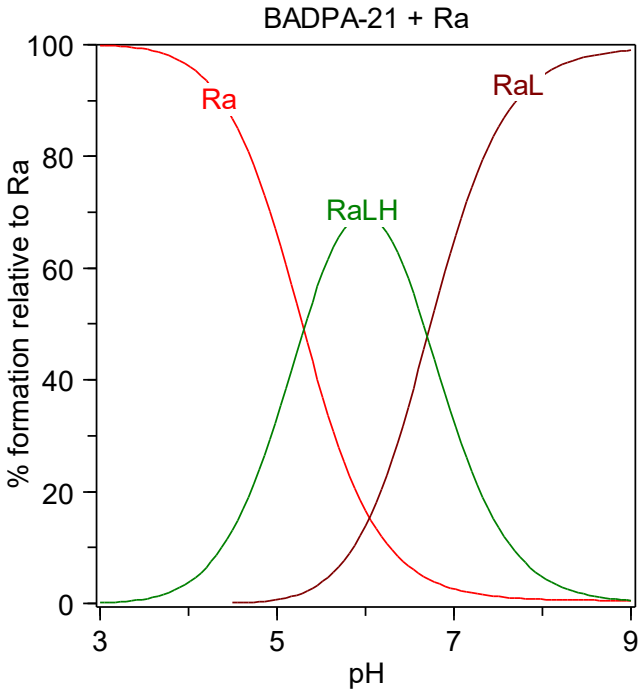

Figure S21. The species distribution diagram for the Ra^{2+} and BADPA-21 system as a function of pH. To make the species distribution diagram of radium species, the average concentrations of Ra^{2+} (0.75 nM) and BADPA-21 (0.1 mM) were used, which had been applied to determine the conditional stability constant.

4. X-ray crystallographic data

Table S3. Crystallographic data for BADPA-21 and [Ba(HBADPA-21)]ClO_4.

	BADPA-21	[Ba(HBADPA-21)]ClO_4
CCDC	2532020	2342556
Empirical formula	$C_{32}H_{62}N_4O_{20}$	$C_{32}H_{39}BaClN_4O_{13}$
Formula weight	822.85	860.46
T (K)	150	100
Crystal system	Triclinic	Monoclinic
Space group	P-1	$P2_1/n$
Z / Z'	2 / 1	4 / 1
a, Å	9.4912(6)	11.6375(7)
b, Å	14.1268(8)	16.5145(9)
c, Å	15.9346(9)	18.4211(11)
α, °	90.628(2)	90
β, °	102.940(2)	100.934(3)
γ, °	100.709(2)	90
V, Å^3	2042.9(2)	3476.0(4)
d_{calc} (g cm^{-3})	1.338	1.644
μ, cm^{-1}	1.11	12.91
F(000)	884	1744
$2\theta_{max}$, °	52.14	58.00
Refls collected	28927	19566
Independent refls [R_{int}]	8067 [0.0584]	9140 [0.0742]
Observed refls [$I > 2\sigma(I)$]	5822	6437
Parameters	565	460
*R*1	0.0606	0.0645
w*R*2	0.1456	0.1643
GOF	1.038	1.031
Residual density, $\Delta\rho_{max}$/ $\Delta\rho_{min}$ (e A^{-3})	0.400/-0.329	3.109/-2.164

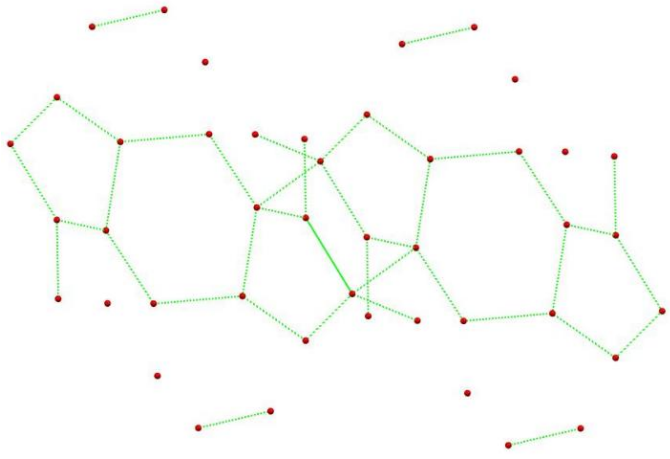

Figure S22. The hydrogen-bonded water clusters in the crystal structure of BADPA-21. Only the oxygen atoms of the water molecules are shown, and lines are drawn only between molecules participating in H-bonds with each other (unconnected molecules and pairs are H-bonded to the macrocycle).

Table S4. Hydrogen bonds for BADPA-21 (Å and °).

D-H...A	Bond length d(D...A)	Bond angle (DHA)
N(1)-H(1N)...O(10)#1	2.768(3)	173
N(2)-H(2N)...O(11)#2	2.807(3)	161
O(10)-H(10C)...O(9)#2	2.838(3)	165
O(10)-H(10D)...O(6)#3	2.930(3)	168
O(11)-H(11C)...O(9)#2	2.932(3)	178
O(11)-H(11D)...O(12)	2.803(4)	159
O(12)-H(12C)...O(8)#4	2.804(3)	175
O(12)-H(12D)...O(6)#3	2.756(3)	166
O(13)-H(13C)...O(8)#5	2.853(3)	164
O(13)-H(13D)...O(7)#6	2.670(3)	161
O(14)-H(14C)...O(15)#7	2.839(3)	173
O(14)-H(14D)...O(13)	2.706(3)	169
O(15)-H(15C)...O(18)#8	2.786(4)	154
O(15)-H(15D)...O(16)#7	2.923(3)	156
O(16)-H(16C)...O(6)#3	2.846(3)	164
O(16)-H(16D)...O(19)	2.796(3)	169
O(17)-H(17C)...O(8)#4	2.836(3)	171
O(17)-H(17D)...O(16)	2.867(3)	177
O(18)-H(18C)...O(17)	2.762(3)	170
O(18)-H(18D)...O(14)	2.722(4)	162
O(19)-H(19C)...O(9)#2	2.772(3)	161
O(19)-H(19D)...O(15)	2.906(3)	153
O(20)-H(20C)...O(3)	2.851(4)	179
O(20)-H(20D)...O(18)#8	2.933(4)	180

Symmetry transformations used to generate equivalent atoms: #1 x,y-1,z; #2 -x+1,-y+1,-z; #3 x,y+1,z; #4 -x+2,-y+1,-z; #5 x,y,z+1; #6 -x+2,-y,-z+1; #7 -x+1,-y+1,-z+1; #8 x-1,y,z.

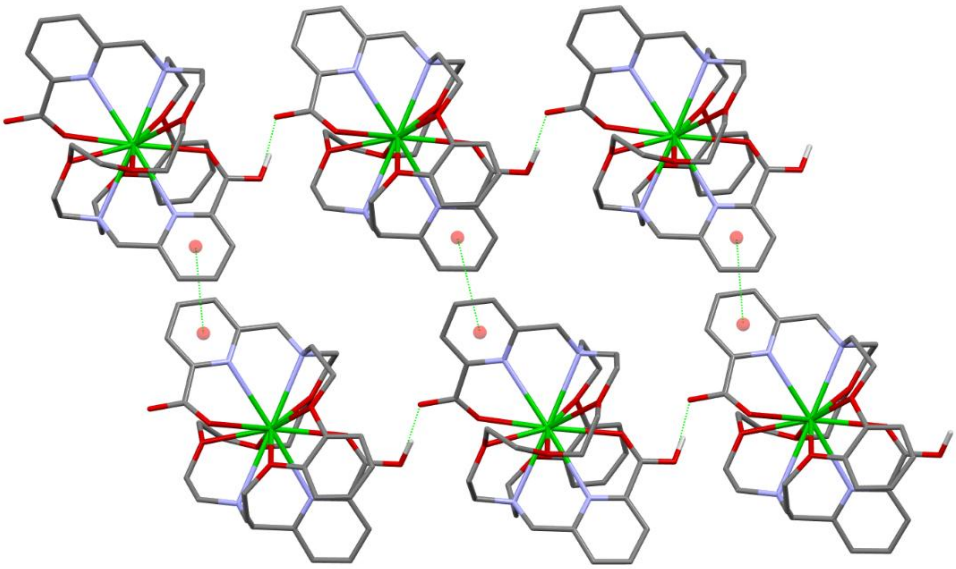

Figure S23. The supramolecular packing motif in the crystal structure of [Ba(HBADPA-21)]ClO_4, built *via* H-bonds between the carboxyl and the carboxylate groups (O7...O9 2.460(6) Å, OHO 170°) and shifted π-stacks (shortest C…C 3.934 Å). Perchlorate anions are not shown.

Table S5. SHAPE 2.1 Output values of the continuous shape measures (CSMs) (five lowest measures for each metal sphere).

Complex					
Ba(HBADPA-21)	JCPAPR-11	JCPPR-11	JAPPR-11	JASPC-11	EBPY-11
	5.068	6.21	6.445	8.917	15.928
Ba(Hmacropa-XL)	JCPAPR-11	JCPPR-11	JASPC-11	JAPPR-11	EBPY-11
(CSD TIXGOA)	3.693	6.642	6.871	8.778	17.511
Ba(Hmacropa)	JCPAPR-11	JASPC-11	JCPPR-11	JAPPR-11	EBPY-11
(CSD BINWUT)	5.017	6.222	6.763	10.795	18.338
Ba(macropa-b-alanine)	JCPAPR-11	JCPPR-11	JASPC-11	JAPPR-11	EBPY-11
(CSD UMAHIC)	5.623	6.340	6.750	9.725	18.068

Abbreviations for 11-coordinated: JCPAPR-11 - capped pentagonal antiprism; JCPPR-11 - capped pentagonal prism; JAPPR-11 - augmented pentagonal prism; JASPC-11 - augmented sphenocorona, EBPY-11 - enneagonal bipyramid.

Table S6. Bond lengths (Å) in metal coordination sphere in the published complexes Ba(Hmacropa) (CSD BINWUT) and Ba(macropa-β-alanine) (CSD UMAHIC) and geometric parameters used for cavity size estimation (Å).

Ba(Hmacropa) (CSD BINWUT)		Ba(macropa-β-alanine) (CSD UMAHIC)	
Ba1-O5	2.809	Ba1-O3	2.768
Ba1-O7	2.784	Ba1-O1	2.743
Ba1-N3	2.930	Ba1-N3	2.940
Ba1-N4	2.932	Ba1-N6	2.915
Ba1-O1	2.834	Ba1-O7	2.882
Ba1-O2	2.883	Ba1-O8	2.924
Ba1-O3	2.846	Ba1-O5	2.924
Ba1-O4	2.882	Ba1-O6	2.916
Ba1-N2	3.014	Ba1-N1	3.050
Ba1-N1	3.006	Ba1-N2	2.995
Ba1-O9	2.925	Ba1-O9	2.782
R_{macro}	2.81	R_{macro}	2.82
R_{total}	2.89	R_{total}	2.90

5. NMR study

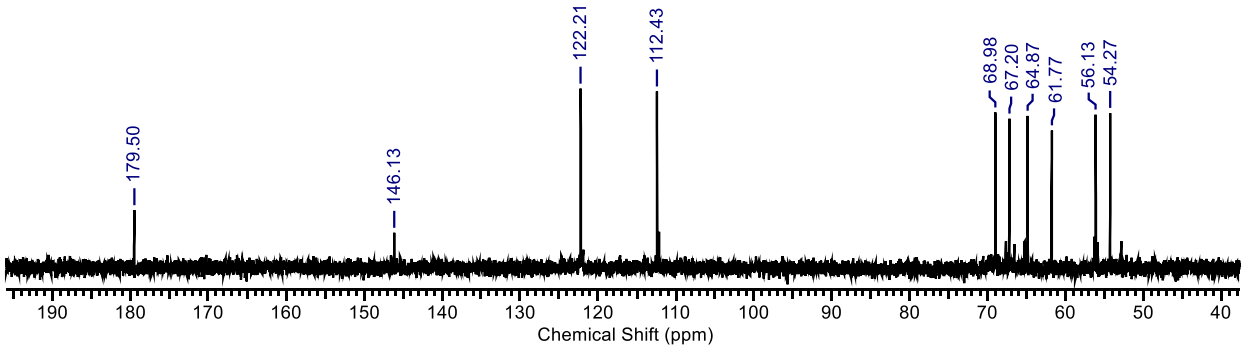

Figure S24. ^{13}C NMR spectrum of the complex Ca(BADA-18) in D_2O.

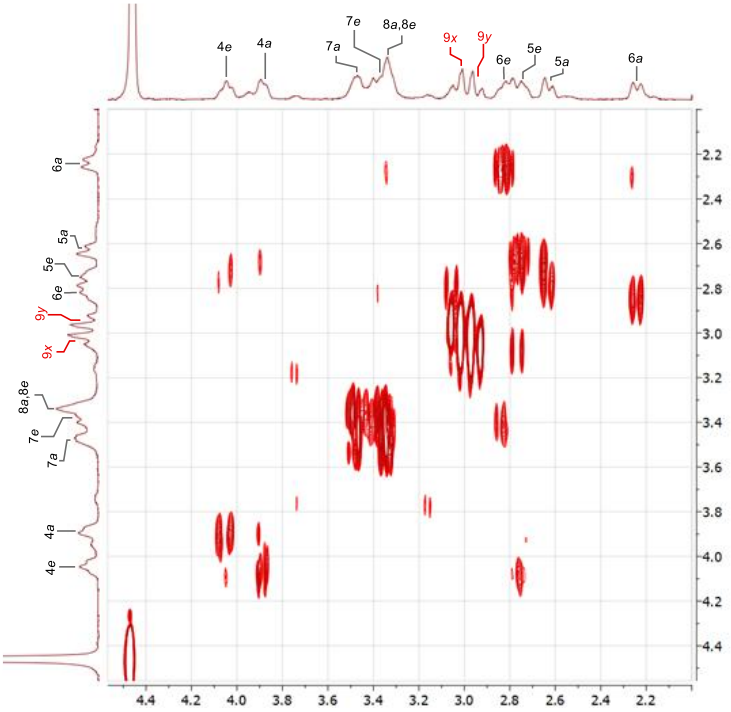

Figure S25. ^{1}H-^{1}H COSY NMR spectrum of the complex Ca(BADA-18) in D_2O (aliphatic region).

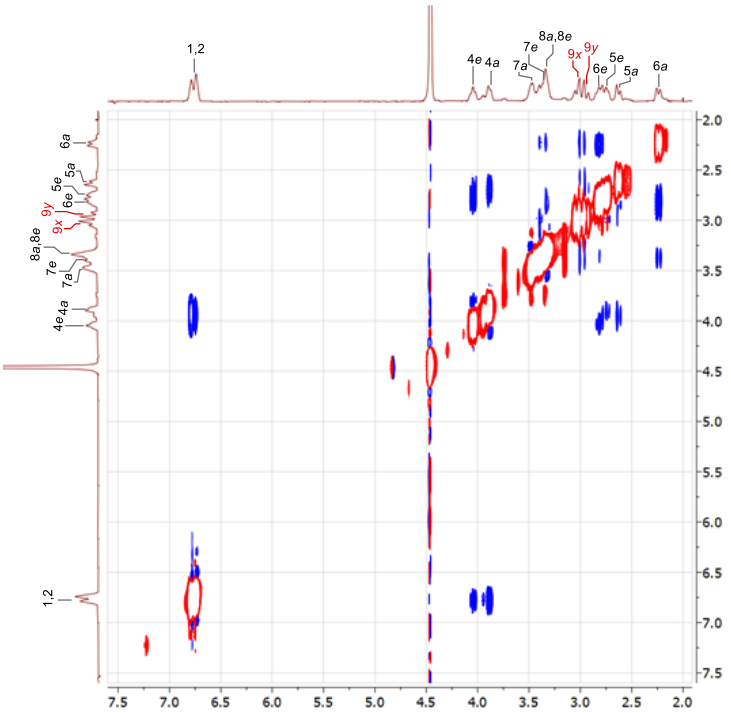

Figure S26. ^{1}H-^{1}H NOESY NMR spectrum of the complex Ca(BADA-18) in D_2O.

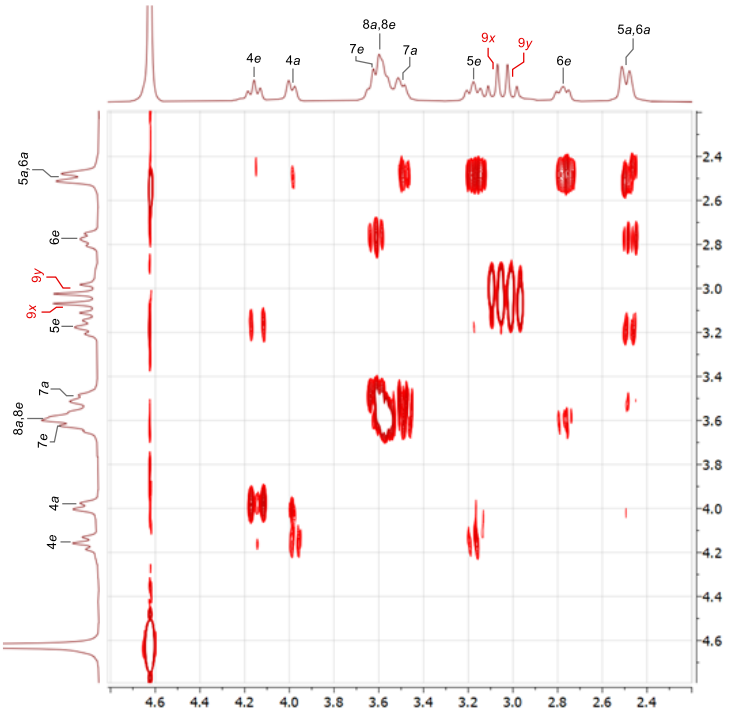

Figure S27. ^{1}H-^{1}H COSY NMR spectrum of the complex Ba(BADA-18) in D_2O (aliphatic region).

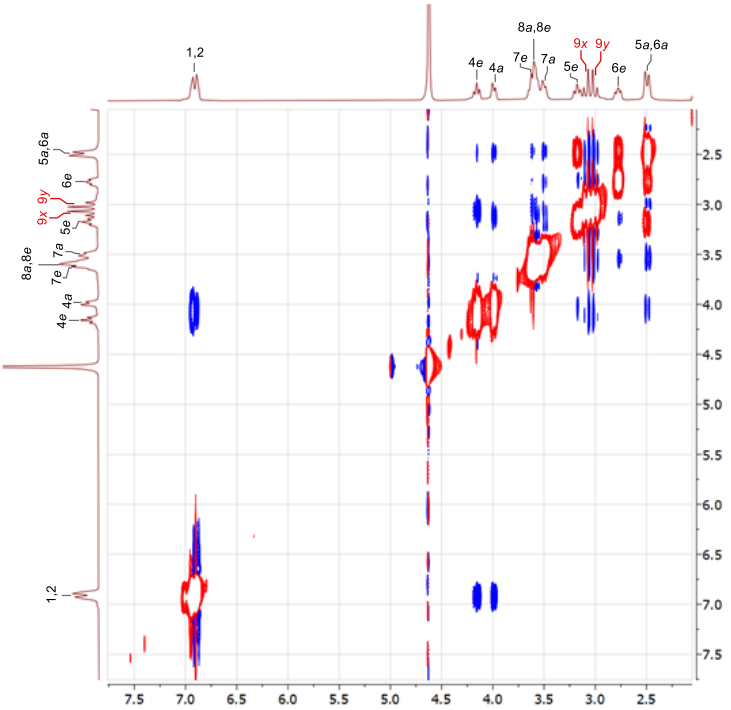

Figure S28. ^{1}H-^{1}H NOESY NMR spectrum of the complex Ba(BADA-18) in D_2O.

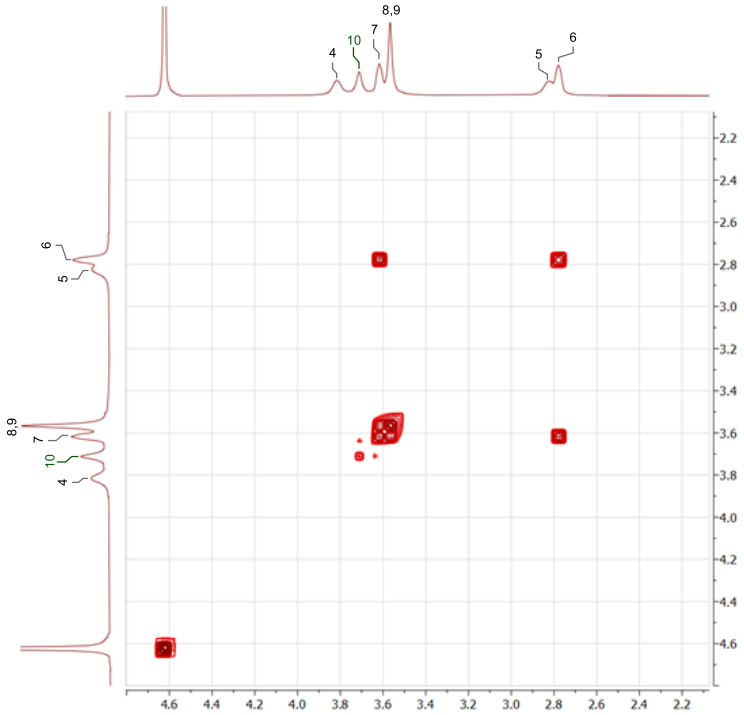

Figure S29. ^{1}H-^{1}H COSY NMR spectrum of the complex Ca(BADPA-21) in D_2O (aliphatic region).

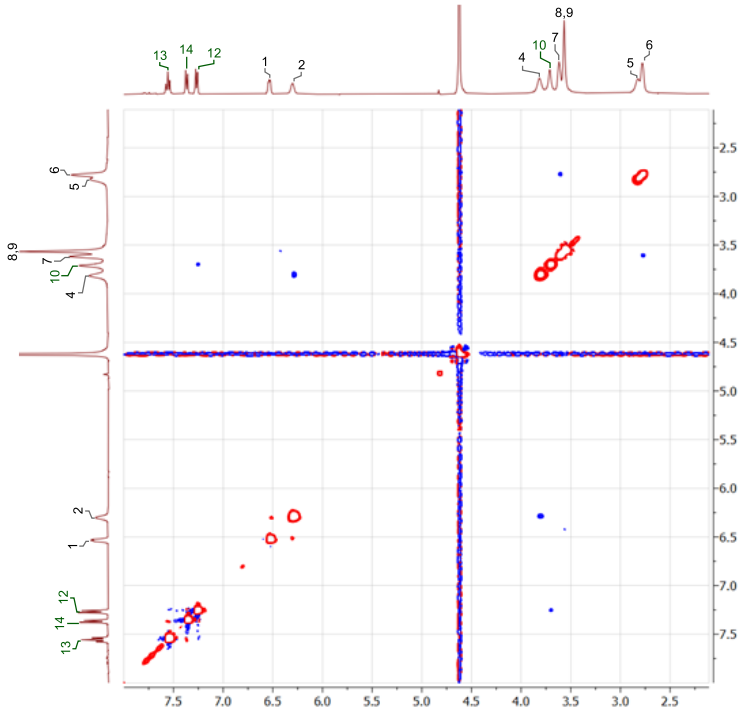

Figure S30. ^{1}H-^{1}H NOESY NMR spectrum of the complex Ca(BADPA-21) in D_2O.

6. Radiolabeling and *in vitro* stability

Table S7. Radiochemical yields (RCY, %) of $[^{226}Ra]Ra^{2+}$ complexes with various chelators (25 °C, 1 min).

c(L)	BADA-18	BADA-21	BADPA-18	BADPA-21	macropa
1 mM	0.2 ± 0.1	2.4 ± 0.4	18 ± 4	99 ± 6	98 ± 7
0.1 mM				60 ± 7	99 ± 8
0.01 mM				5 ± 3	46 ± 7

Table S8. Radiochemical stability (%) of $[^{226}Ra]Ra^{2+}$ complexes and $[^{226}Ra]Ra^{2+}$ (blank) in FBS (37 °C, *c*(L) = 1 mM, *V*(complex) / *V*(FBS) = 1/9). Values represent the percentage of intact complex or, for the blank, the percentage of $[^{226}Ra]Ra^{2+}$ unbound to serum proteins.

Time	$[^{226}Ra]Ra^{2+}$ (blank)	$[^{226}Ra]Ra$(BADPA-21)	$[^{226}Ra]Ra$(macropa)
1 min	1.2 ± 0.4		
1 hour		103 ± 6	102 ± 9
3 hours		100 ± 10	100 ± 8
6 hours	0.3 ± 0.1		
1 day		106 ± 8	103 ± 8
2 days		98 ± 6	98 ± 8
11 days		85 ± 8	87 ± 6

Table S9. Radiochemical stability (%) of $[^{226}Ra]Ra^{2+}$ complexes in the presence of biologically relevant metal ions (37 °C, 1 day).

M^{n+}	*c*(M^{n+}), mM	$[^{226}Ra]Ra$(BADPA-21)	$[^{226}Ra]Ra$(macropa)
Ca^{2+}	5	95 ± 2	97 ± 3
Zn^{2+}	0.1	104 ± 13	98 ± 1
Mg^{2+}	5	97 ± 2	100 ± 2
Cu^{2+}	0.1	97 ± 2	101 ± 5
Na^{+}	150	98 ± 1	102 ± 4